Radiotherapy and Oncology 140 (2019) 175–181

Contents lists available at ScienceDirect

Radiotherapy and Oncology

journal homepage: www.thegreenjournal.com

Original Article

Optic nerve constraints for carbon ion RT at CNAO – Reporting and relating outcome to European and Japanese RBE

Jon Espen Dale [a,b,*], Silvia Molinelli [c], Viviana Vitolo [c], Barbara Vischioni [c], Maria Bonora [c], Giuseppe Magro [c], Helge Egil Seime Pettersen [a], Andrea Mairani [c,d], Azusa Hasegawa [c,e], Olav Dahl [a,b], Francesca Valvo [c], Piero Fossati [c,f]

[a] Department of Oncology and Medical Physics, Haukeland University Hospital, Bergen; [b] Department of Clinical Science, Faculty of Medicine, University of Bergen, Norway; [c] National Center of Oncological Hadrontherapy, Pavia, Italy; [d] Heidelberg Ion-Beam Therapy Center, Heidelberg, Germany; [e] Osaka Heavy Ion Therapy Center, Osaka, Japan; [f] MedAustron Ion Therapy Center, Wiener Neustadt, Austria

ARTICLE INFO

Article history:
Received 11 March 2019
Received in revised form 18 June 2019
Accepted 18 June 2019
Available online 13 July 2019

Keywords:
Carbon ion radiotherapy
Optic nerve
Relative biological effectiveness
Organs at risk
Vision disorders
Long term adverse effects

ABSTRACT

Background and purpose: Until now, carbon ion RT (CIRT) dose constraints for the optic nerve (ON) have only been validated and reported in the NIRS RBE-weighted dose (D_{NIRS}). The aim of this work is to improve CNAO's RBE-weighted dose (D_{LEM}) constraints by analyzing institutional toxicity data and by relating it to D_{NIRS}.

Material and methods: A total of 65 ONs from 38 patients treated with CIRT to the head and neck region in the period 2013–14 were analyzed. The absorbed dose (D_{Abs}) of the treatment plans was reproduced and subsequently both D_{LEM} and D_{NIRS} were applied, thus relating CNAO clinical toxicity to D_{NIRS}.

Results: Median FU was 47 (26–67) months. Visual acuity was preserved for the 56 ONs in which the old constraints were respected. Three ONs developed visual decline at $D_{LEM|1\%} \geq 71$ Gy(RBE)/$D_{LEM|20\%} \geq 68$ Gy (RBE), corresponding to $D_{NIRS|1\%} \geq 68$ Gy(RBE)/$D_{NIRS|20\%} \geq 62$ Gy(RBE). Dose recalculation revealed that NIRS constraints of $D_{NIRS|1\%} \leq 40$ Gy(RBE)/$D_{NIRS|20\%} \leq 28$ Gy(RBE) corresponded to $D_{LEM|1\%} \leq 50$ Gy(RBE)/$D_{LEM|20\%} \leq 40$ Gy(RBE). Reoptimization of treatment plans with these new D_{LEM} constraints showed that the dose distribution still complied with NIRS constraints when evaluated in D_{NIRS}. However, due to uncertainties in the method, and to comply with the EQD2-based constraints used at GSI/HIT, a more moderate constraint relaxation to $D_{LEM|1\%} \leq 45$ Gy(RBE)/$D_{LEM|20\%} \leq 37$ Gy(RBE) has been implemented in CNAO clinical routine since October 2018.

Conclusion: New D_{LEM} constraints for the ON were derived by analyzing CNAO toxicity data and by linking our results to the experience of NIRS and GSI/HIT. This work demonstrates the value of recalculating and reporting results in both D_{LEM} and D_{NIRS}.

In order to optimize carbon ion radiotherapy (CIRT) there is a need to validate dose constraints for important organs at risk (OARs). For the optic nerve (ON), constraints have been validated by the *National Institute of Radiobiological Sciences* (NIRS, Japan) [1], in which the *relative biological effectiveness* (RBE) for CIRT has been predicted by the *mixed beam model* (RBE_{NIRS}) [2,3], and have been reported as the *NIRS RBE-weighted dose* (D_{NIRS}). The NIRS constraints are not immediately useful for European centers where the *Local effect model I* (RBE_{LEM})[4,5] is used, because comparative studies show that RBE_{LEM} can predict a 60% higher RBE in the entrance region of the beam [6], and 5–15% higher RBE in the spread-out Bragg peak [7–9], relative to RBE_{NIRS}. At the *National Center of Oncological Hadrontherapy* (CNAO, Italy) [10,11], dose constraints for ONs complied nominally with the NIRS constraints: $D_{1\%} \leq 40$ Gy(RBE) and $D_{20\%} \leq 28$ Gy(RBE), although RBE_{LEM} is used in treatment plan optimization. This was a conservative approach, adopted at the beginning of clinical activity to minimize the risk of unexpected visual impairment due to lack of clinically validated RBE_{LEM}-weighted dose (D_{LEM}) constraints. The aim of this work was to improve CNAO's ON dose constraints by analyzing institutional toxicity and by relating the results to the constraints validated by NIRS.

* Corresponding author at: Department of Oncology and Medical Physics, Haukeland University Hospital, PB 1400, 5021 Bergen, Norway.
E-mail address: jon.espen.dale@helse-bergen.no (J.E. Dale).

https://doi.org/10.1016/j.radonc.2019.06.028
0167-8140/

Material and methods

Patient selection

We identified a total of 38 patients (65 ONs) who had been treated at CNAO in the period 2013–14 with CIRT to the head and neck region and who had:

- at least 2 years of follow-up.
- maximum dose ($D_{LEM|1\%}$) >20 Gy(RBE) to optic nerve.
- available records of visual acuity before and after CIRT.

and did not have:

- radiotherapy before or after CIRT at CNAO.
- higher dose to the chiasm than to the optic nerve.
- preexisting visual impairment.
- development of visual impairment in the follow-up period due to other causes than radiation induced optic pathway neuropathy (e.g. recurrent tumor, etc.).

Carbon ion radiotherapy at CNAO

All patients were treated to a prescribed D_{LEM} of 68.8 or 70.4 Gy (RBE) in 16 fractions (4 fractions/week) using the *syngo*® RT Planning (Siemens Healthcare, Erlangen, Germany) treatment planning system (TPS). The patients were included in prospective protocols (CNAO S9/2012/C, CNAO S12/2012/C and CNAO S15/2012/C) approved by the regional ethics committee, and signed consent was required for participation. Dose constraints for the ONs and chiasm were $D_{LEM|1\%} \leq 40$ Gy(RBE) and $D_{LEM|20\%} \leq 28$ Gy(RBE). A 2 mm margin was applied to the planning organ at risk volume (PRV) in which the dose constraints, for plan optimization purposes, were $D_{LEM|1\%} \leq 60$ Gy(RBE) and $D_{LEM|20\%} \leq 40$ Gy(RBE). Following the patient's consent, the constraints could be exceeded if they prevented adequate dose coverage to the target volume, provided that the function of the contralateral ON was adequate and would be preserved.

Follow-up

Patients were followed at CNAO every 3rd month with a clinical examination and magnetic resonance imaging (MRI). If symptoms of visual defects were reported by the patient or detected on clinical examination, the patient was referred to an ophthalmologist for further investigations and diagnosis. *Radiation induced optic neuropathy* (RION) was scored according to the *Optic Nerve Disorder* term of the *Common Terminology Criteria for Adverse Events version 4.03* (CTCAE) [12].

Recalculation to RBE_{NIRS}-weighted dose distributions

The patients' computer tomography (CT) image files, structure set files, dose files and plan files (DICOM files) were exported from *syngo*® TPS and imported to the *matRad* open source multimodality radiation TPS (https://e0404.github.io/matRad/) in which the absorbed dose (D_{Abs}) and D_{LEM} were reproduced. Dose–volume histograms (DVHs) of targets and OARs were compared with the corresponding DVHs of the dose distribution from the *syngo*® TPS to ensure correct reproduction of both D_{Abs} and D_{LEM} (results not reported). Secondly, the RBE_{NIRS} was implemented in the matRad TPS code and D_{NIRS} was derived from the exact same absorbed dose. This enabled a direct comparison of each patient's D_{LEM} and D_{NIRS} based exclusively on the differences in the RBE modeling.

Statistics and normal tissue complication probability (NTCP) modeling

Differences in frequencies between cohorts were compared using Chi-Square test or Fischer's exact test. Non-parametrical distributions were compared with the Mann–Whitney *U*-test, while normally distributed data were compared with the independent samples *T*-test. NTCP was calculated for cumulative DVH variables $D_{1\%}$, $D_{10\%}$, $D_{20\%}$ through $D_{50\%}$ and were used to derive the dose that would result in 5% (TD5) and 50% (TD50) probability of RION according to the equation:

$$\mathrm{NTCP}(Dx\%) = 1 - \frac{1}{1 + e^{a+b*d}}$$

where d is the RBE-weighted dose to $x\%$ of the ON volume and a and b are constants estimated to provide the best fit to the data set, using binary logistic regression. All statistical procedures were performed with the software IBM SPSS Statistics for Windows, Version 24.0 (IBM Corp., Armonk, NY, U.S.A.). All *p*-values were obtained from two-sided tests. *P*-values <0.05 were considered significant.

Reoptimization of treatment plans with new set of constraints

Finally, a subset of patients, in which the original constraints had caused inadequate dose coverage to the clinical target volume (CTV) in their original D_{LEM} plan, was reoptimized with the RayStation® 7.0 TPS (RaySearch Laboratories AB, Stockholm, Sweden) (currently under commissioning at CNAO) applying RBE_{LEM} as RBE model and optimizing the plan with a new set of D_{LEM} constraints, as proposed by this work (see *Results*). Subsequently, also these plans were recalculated to D_{NIRS}, to validate that the reoptimized ON DVHs still complied with the original NIRS constraints.

A flow chart of the steps involved in our method is presented in Appendix A, Fig. A1.

Results

Patient and disease characteristics are presented in Table 1. Median follow-up time was 47 (range 26–67) months. Among the 38 patients and 65 ONs analyzed, toxicity did not occur in the 52 ONs in which the current constraints were respected. Three patients developed unilateral RION (all CTCAE grade 4) at doses $D_{LEM|1\%} \geq 71$ Gy(RBE)/$D_{NIRS|1\%} \geq 68$ Gy(RBE) and $D_{LEM|20\%} \geq 68$ Gy (RBE)/$D_{NIRS|20\%} \geq 62$ Gy (RBE). In all these cases, the ON constraints were intentionally violated in order to achieve adequate dose coverage to the nearby tumor. RION was detected at 11, 29 and 42 months after completed CIRT. In addition to the 3 ONs that developed toxicity, the applied constraints were breached for 10 ONs with a median follow-up of 45 (range 26–50) months. When evaluating the DVHs with D_{NIRS}, only 6 of these ONs still exceeded NIRS constraints. All individual ONs in both D_{LEM} and D_{NIRS} are presented in Fig. 1, demonstrating that RBE_{NIRS} generally predicts lower RBE than RBE_{LEM}, resulting in the DVHs being shifted toward lower doses. Key dosimetric data are presented in Table 2.

The relationship of D_{NIRS} and D_{LEM} for $D_{1\%}$ and $D_{20\%}$ is presented in Fig. 2, showing that a $D_{NIRS|1\%}$ of ≤ 40 Gy(RBE) and a $D_{NIRS|20\%}$ of ≤ 28 Gy(RBE) could approximately be translated into new CNAO constraints of $D_{LEM|1\%} \leq 50$ Gy(RBE) and $D_{LEM|20\%} \leq 40$ Gy(RBE). These new constraints for D_{LEM} are plotted as open red squares in Fig. 1. As can be observed, the ONs that comply with the original NIRS constraints when their DVHs are evaluated in D_{NIRS}, remain compliant with the new CNAO constraints when their DVHs are evaluated in D_{LEM}. Likewise, the ONs that exceed the NIRS constraints when evaluated in D_{NIRS} still exceed the new CNAO constraints when evaluated in D_{LEM}.

The estimates of TD5 and TD50 for parameters D1%–D50%, and their relation to the same parameters from the dose constraint val-

Table 1
Patient and disease characteristics for all patients and grouped by patients that developed (*RION = yes*) or did not develop (*RION = no*) radiation induced optic neuropathy.

		All (n = 38)	RION = yes (n = 3)	RION = no (n = 35)
Sex, female:male		18:20	2:1	16:19
Median age (range), y		59 (16–81)	62 (54–68)	54 (16–81)
Comorbidity, n (%)				
	Hypertension	9 (23.7%)	1 (33.3%)	8 (22.9%)
	Diabetes mellitus	8 (21.1%)	1 (33.3%)	7 (20.0%)
	Cardiovascular disease	4 (10.5%)	1 (33.3%)	3 (8.6%)
Histology, n (%)				
	Adenoid cystic carcinoma	14 (36.8%)	2 (66.7%)	12 (34.3%)
	Chordoma	14 (36.8%)	0 (0.0%)	14 (40.0%)
	Chondrosarcoma	3 (7.9%)	0 (0.0%)	3 (8.6%)
	Other sarcoma	5 (13.2%)	1 (33.3%)	4 (11.4%)
	Acinar cell carcinoma	1 (2.6%)	0 (0.0%)	1 (2.9%)
	Mucosal malignant melanoma	1 (2.6%)	0 (0.0%)	1 (2.9%)
Site, n (%)				
	Clivus	12 (31.6%)	1 (33.3%)	11 (31.4%)
	Paranasal sinus	9 (23.7%)	2 (66.7%)	7 (20.0%)
	Skull base	9 (23.7%)	0 (0.0%)	9 (25.7%)
	Nasal cavity	4 (10.5%)	0 (0.0%)	4 (11.4%)
	Nasopharynx	2 (5.2%)	0 (0.0%)	2 (5.7%)
	Other	2 (5.2%)	0 (0.0%)	2 (5.7%)

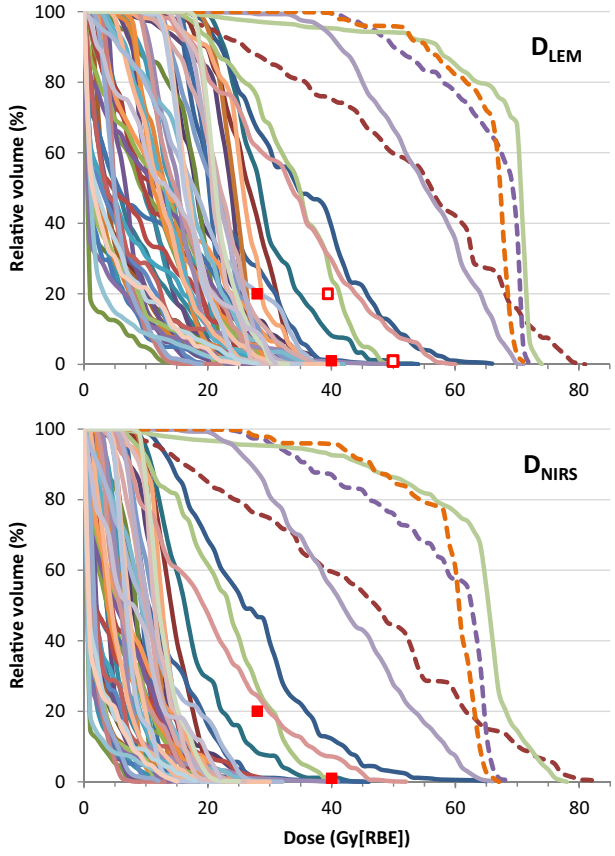

Fig. 1. Cumulative DVH of all 65 ONs in D_{LEM} (upper panel) and D_{NIRS} (lower panel). Dashed DVH-lines represent optic nerves that developed RION. Red, filled squares indicate the current dose constraints of $D_{1\%}$ ≤40 Gy(RBE) and $D_{20\%}$ ≤28 Gy(RBE). Red, open squares in upper panel represent possible new D_{LEM} constraints for CNAO based on RBE-weighted dose translation.

idation at NIRS [1] are presented in Table 3, showing a remarkable agreement of TD50 between NIRS and CNAO data in D_{NIRS}, while estimates of TD5 are substantially higher when based on the CNAO data.

The NIRS validation cohort consisted of 30 patients (54 ONs), in which visual impairment occurred in 9 patients (11 ONs). All ON DVHs from this cohort are displayed in Fig. 3 (black DVHs). The DVHs of the ONs developing toxicity in the CNAO cohort (in D_{NIRS}) are superimposed in red, showing good agreement to the NIRS cohort in respect to the dose levels at which toxicity seems to develop. The figure also displays the TD50 and TD5 estimates from Table 3, demonstrating the coherency of TD50 values and the discrepancy in TD5 values between the cohorts.

A subset of patients in which the current constraints hindered adequate dose coverage to the clinical target volume (CTV) was reoptimized applying the proposed new set of D_{LEM} constraints, i.e. $D_{LEM|1\%}$ ≤50 Gy(RBE) and $D_{LEM|20\%}$ ≤40 Gy(RBE). After recalculation of the new plan to D_{NIRS}, the ON DVHs consistently remained compliant to the original NIRS constraints. The dose distributions of a representative patient, in which the right ON needed to be spared in order to avoid bilateral blindness, are shown in Fig. 4. The conservative constraints applied in the original plan inevitably resulted in inadequate dose coverage to the part of the CTV adjacent to the right ON (Fig. 4A). Post hoc recalculation of the plan to D_{NIRS} (Fig. 4B) suggests that the right ON was excessively spared relative to the NIRS validated constraints. Reoptimizing the plan with the new D_{LEM} constraints significantly improves CTV coverage (Fig. 4C-D vs. A-B) while maintaining compliance with the NIRS validated constraints in respect to D_{NIRS} (Fig. 4D). In this patient, the reoptimized plan achieved a dose coverage in which 99% of the prescribed dose covered 92% of the CTV and 95% of the prescribed dose covered 97.7% of the CTV. The respective dose coverage to the CTV of the original plan was only 82% and 93.2%.

Discussion

Due to the many uncertainties involved in the prediction of the RBE of CIRT, there will inevitably be substantial uncertainties related to the extrapolation of OAR constraints from the experience of photon RT. Therefore, the strategy of CNAO has been to define OAR constraints for CIRT based on CIRT clinical data. To date, there is a general lack of validated constraints for most OARs. The few publications addressing this topic have all reported the dose statistics and NTCPs solely in the respective institutional RBE-weighted dose [1,13–18], thus making them incomprehensible to institutions applying a different RBE model.

Table 2
Dose statistics for all ONs and/or grouped by ONs that developed (*RION = yes*) or did not develop (*RION = no*) radiation induced optic neuropathy. *P* values represent the significance level for the observed difference in variable distribution between *RION = yes* and *RION = no* groups.

	All (n = 65)	RION = yes (n = 3)	RION = no (n = 62)	*P* value
Median ON volume (range), cm^3	0.92 (0.45–1.52)	0.74 (0.46–1.34)	0.94 (0.45–1.52)	0.485
D1%, median (range)				
D_{LEM}, Gy (RBE)		71.6 (70.7–78.6)	28.4 (12.2–73.6)	<0.001
D_{NIRS}, Gy (RBE)		67.2 (66.3–79.3)	18.1 (6.1–76.2)	<0.001
D10%, median (range)				
D_{LEM}, Gy (RBE)		70.8 (69.1–72.5)	22.9 (6.5–71.8)	<0.001
D_{NIRS}, Gy (RBE)		65.2 (63.8–70.0)	12.8 (3.0–71.8)	<0.001
D20%, median (range)				
D_{LEM}, Gy (RBE))		68.5 (68.1–70.5)	19.5 (0.7–71.4)	<0.001
D_{NIRS}, Gy (RBE)		63.0 (61.8–64.7)	10.2 (0.2–68.2)	<0.001
D30%, median (range)				
D_{LEM}, Gy (RBE)		68.1 (62.6–70.1)	17.1 (0.2–71.1)	<0.001
D_{NIRS}, Gy (RBE)		62.2 (54.6–64.2)	8.4 (0.0–66.7)	<0.001
D50%, median (range)				
D_{LEM}, Gy (RBE)		67.4 (56.1–69.3)	12.6 (0.1–70.7)	<0.001
D_{NIRS}, Gy (RBE)		60.4 (47.3–62.6)	5.6 (0.0–65.4)	<0.001

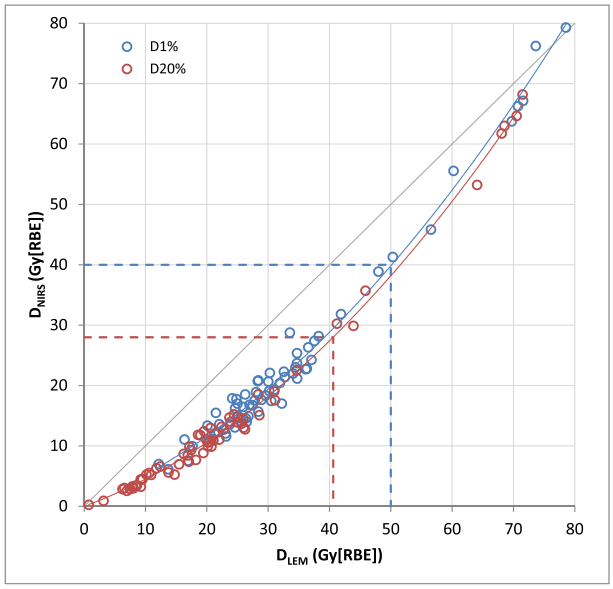

Fig. 2. Relationship of D_{NIRS} and D_{LEM} for $D_{1\%}$ (blue circles) and $D_{20\%}$ (red circles) with corresponding trend lines. Dashed lines represent translation from D_{NIRS} to D_{LEM} for constraint $D_{1\%}$ (blue) and $D_{20\%}$ (red).

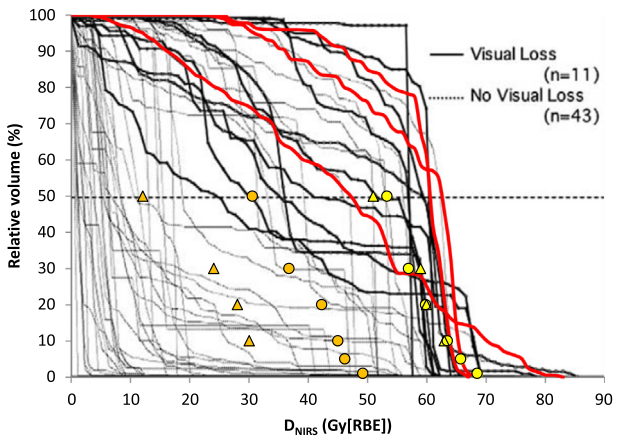

Fig. 3. Reprint of Fig. 4a from Hasegawa et al. [1] showing the DVHs from the NIRS validation cohort, where black DVHs represent ONs that developed RION, and gray DVHs represent ONs that did not develop RION. Superimposed on the figure are the D_{NIRS} DVHs (red) of the three ONs from the CNAO cohort that developed RION, TD5 (orange) and TD50 (yellow) of NIRS cohort (triangles) and CNAO cohort (circles).

Table 3
TD5 and TD50 values for optic nerve DVH parameters as derived from the present study (CNAO), presented in D_{LEM} and D_{NIRS}, compared to corresponding values reported by Hasegawa et al. [1] (NIRS).

		CNAO		NIRS	*CNAO/NIRS-1 (D_{NIRS})*
		D_{LEM}	D_{NIRS}	D_{NIRS}[a]	
TD5, Gy(RBE)	D1%	62	49	n.s.	
	D10%	61	45	30*	50.0%
	D20%	55	42	28*	50.0%
	D30%	47	37	24*	54.2%
	D50%	41	30	12*	150.0%
TD50, Gy(RBE)	D1%	71	68	n.s.	
	D10%	69	63	63	0.0%
	D20%	66	60	60*	0.0%
	D30%	64	57	59	−3.4%
	D50%	61	53	51	3.9%

n.s. = not specified.
[a] Doses as reported in Hasegawa et al. [1].
* Approximated from Fig. 7 in Hasegawa et al. [1].

The aim of this work was first and foremost to establish less conservative constraints for the ON which could be used at CNAO for a 16 fraction CIRT treatment in which RBE_{LEM} is applied. Our data show that the original constraints have been conservative, resulting in no unanticipated toxic events and with a seemingly large buffer zone separating these constraints and the dose levels where toxicity was observed. In NTCP modeling, we found TD50 to agree well with the published TD50 estimates at NIRS, while there was a discrepancy in TD5 estimates. This discrepancy is probably a result of a scarcity of observations in the CNAO cohort in the middle to high doses, relative to the NIRS cohort, which is evident when comparing the neatly scattered DVHs of Fig. 3 (NIRS DVHs) to the DVHs of Fig. 1 (CNAO DVHs) which are clustered at lower doses. As a consequence the TD5 estimates of the CNAO data may be unreliable. However, by recalculating our data to D_{NIRS}, it was possible to translate the constraints validated at NIRS into D_{LEM} and thereby propose new CNAO constraints to be evaluated for feasibility. As shown in *Results*, new CNAO constraints of $D_{LEM|1\%} \leq 50$ Gy(RBE) and $D_{LEM|20\%} \leq 40$ Gy(RBE) seem to correspond well with the NIRS validated constraints.

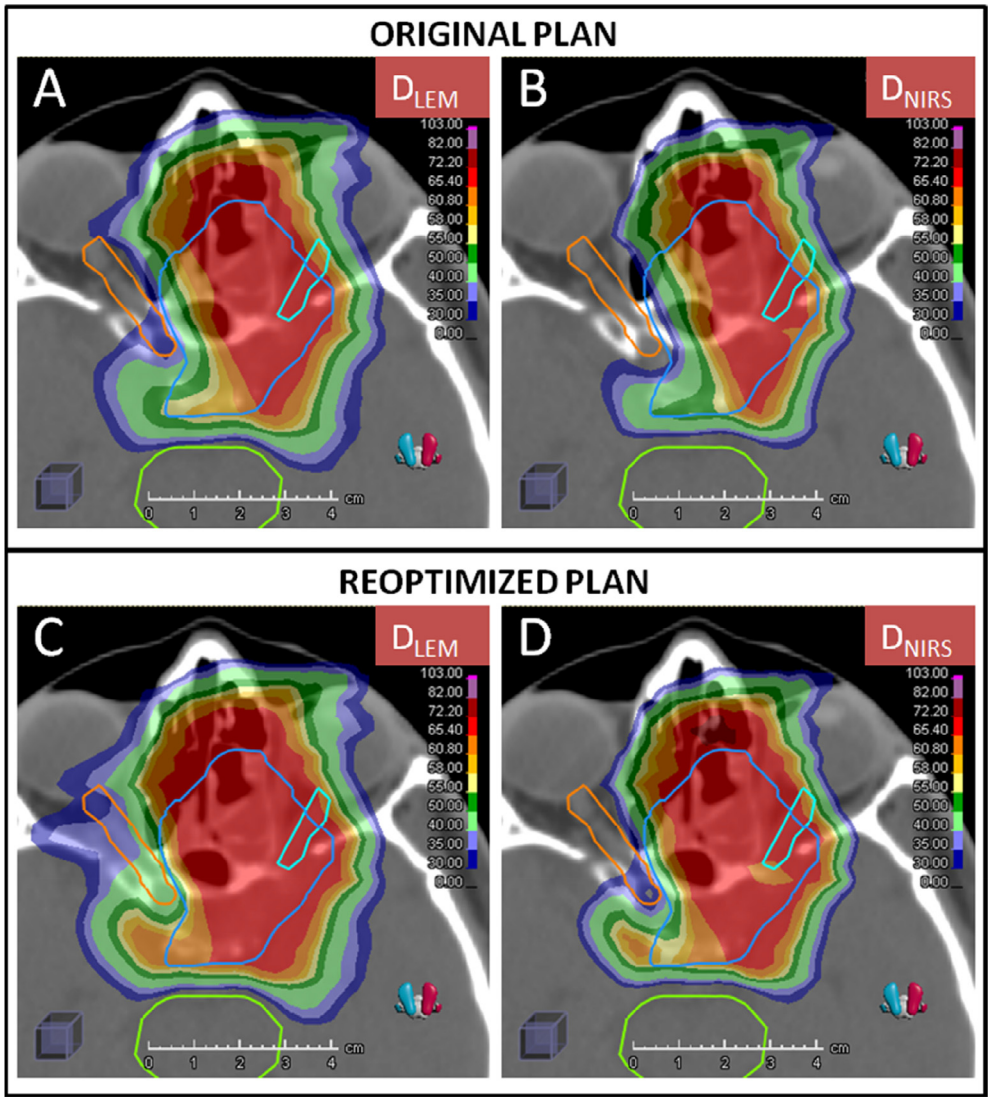

Fig. 4. Original and reoptimized plan in D_{LEM} and D_{NIRS}, demonstrating improved CTV (*blue contour*) dose coverage when applying the new D_{LEM} constraints (Fig. 4c) to the right ON (*orange contour*) and maintained compliance to original NIRS constraints after recalculation to D_{NIRS} (Fig. 4d). Legend for dose distribution in Gy(RBE): *dark blue* = 30–35; *light blue* = 35–40; *light green* = 40–50; *dark green* = 50–55; *yellow* = 55–58; *light orange* = 58–61; *dark orange* = 61–65; *red* = 65–72.

It should be noted that this approach assumes a perfect agreement between the D_{NIRS} recalculated for our cohort, and the D_{NIRS} reported for the validation cohort at NIRS. This may not be correct, since the CIRT at NIRS is delivered by a passive scattering system and with a different beam model calculating the underlying absorbed dose. It has been shown that the absorbed dose of a given RBE-weighted dose could on average vary about 2.5% in the *target region* of head and neck treatments, depending on the beam model [8]. Differences in *out-of-target* areas have not been described in detail, but one might expect to find similar or even more profound deviations in absorbed dose especially within the lateral penumbra dose fall-off. This region is indeed very sensitive to how the lateral spread of the beam is modeled. This is of importance, since the sharp lateral penumbra of the carbon ion beam typically is utilized to avoid high doses to optic nerves located close to the tumor.

Therefore, it is also valuable to relate our proposed new constraints to the traditions of *GSI Helmholtzzentrum für Schwerionenforschung* (GSI), Darmstadt, Germany, later adapted at the *Heidelberg Ion-Beam Therapy center* (HIT), Heidelberg, Germany [19], which together are Europe's most experienced heavy ion therapy center. Their ON constraint has been a maximum dose ($D_{LEM|max}$) of $\leq$54 Gy(RBE), expressed as the *biologically equivalent dose in 2 Gy(RBE) fractions* (EQD2), applying $\alpha/\beta = 2$ Gy [20]. Although GSI/HIT, as CNAO, applies both active scanning beam delivery and the RBE_{LEM} as their RBE model, direct comparison to CNAO is hampered by a difference in fractionation scheme. Typically, HIT uses 20 fractions of 3 Gy(RBE) delivered within 3–3.5 weeks [20,21], while CNAO uses 16 fractions of 4.3–4.4 Gy (RBE) delivered within 4 weeks. Unfortunately, a validation of the GSI/HIT constraint has not yet been published. However, of interest is their published observation of a patient developing bilateral blindness after receiving a nominal $D_{LEM|max}$ of 54 Gy(RBE) to the optic pathways, corresponding to an EQD2 of 63 Gy(RBE) [20]. This raises concern that our proposed new CNAO constraint of $D_{LEM|1\%}$ $\leq$50 Gy(RBE) might be too high, since it converts into an EQD2 of as much as 64 Gy(RBE). Although the application of EQD2 and the use of $\alpha/\beta = 2$ Gy for optic pathways are supported by the European Particle Therapy Network (EPTN) also for proton RT [22], this method may not be sufficiently precise for CIRT, due to the greater uncertainties involved in RBE prediction. However, to our knowl-

edge this approach has been implemented without unanticipated toxicity at GSI/HIT, thus supporting the feasibility of using EQD2 conversion within an institution applying RBE_{LEM}. Accordingly, within the 16 fraction regimen at CNAO, an EQD2 constraint of $\leq$54 Gy(RBE) corresponds to a nominal $D_{LEM|1\%}$ to the ON of $\leq$45 Gy(RBE), and implies a 9% reduction relative to the initial proposal of $D_{LEM|1\%}$ $\leq$50 Gy(RBE). A proportionately equal reduction in the proposed $D_{LEM|20\%}$ constraint results in $D_{LEM|20\%}$ $\leq$37 Gy(RBE).

Regardless of the validity of EQD2 for CIRT, a reduction in the initially proposed new CNAO constraints mitigates the uncertainties involved in our D_{LEM} to D_{NIRS} translation, and is therefore a reasonable first step for dose constraint relaxation at CNAO. As a consequence of the results and deliberations presented in this paper, new ON constraints of $D_{LEM|1\%}$ $\leq$45 Gy(RBE) and $D_{LEM|20\%}$ $\leq$37 Gy(RBE) have been implemented at CNAO since October 2018.

This paper demonstrates the value of assessing and reporting data on CIRT clinical toxicity in both the institution's native RBE model and the alternative model which is widely used clinically. To date, dose recalculation has been a cumbersome affair, but we anticipate that the introduction of such functionality in commercial TPS' within the next years will facilitate this process. We therefore hope that future publications will report OAR dose statistics and NTCPs in both D_{NIRS} and D_{LEM}, and thus accelerate the much needed validation of OAR constraints for both RBE models.

We have derived new and safe dose constraints for the ON to be used at CNAO by analyzing the available institutional data and by mitigating the uncertainties caused by a rather small sample size linking our results to the experience and traditions of NIRS and GSI/HIT. This work also demonstrates how valuable and much needed dose–response data can be saved from being lost in translation between Japanese and European CIRT institutions by recalculating and reporting results in both clinically applied RBE models.

Declaration of Competing Interest

None of the authors have any disclosures or conflicts of interest.

Acknowledgement

Supported by grants from the Trond Mohn Foundation, *Ytre-bygdsvegen 215, Kokstad, Postboks 7150, 5020 BERGEN, Norway.*

Appendix A

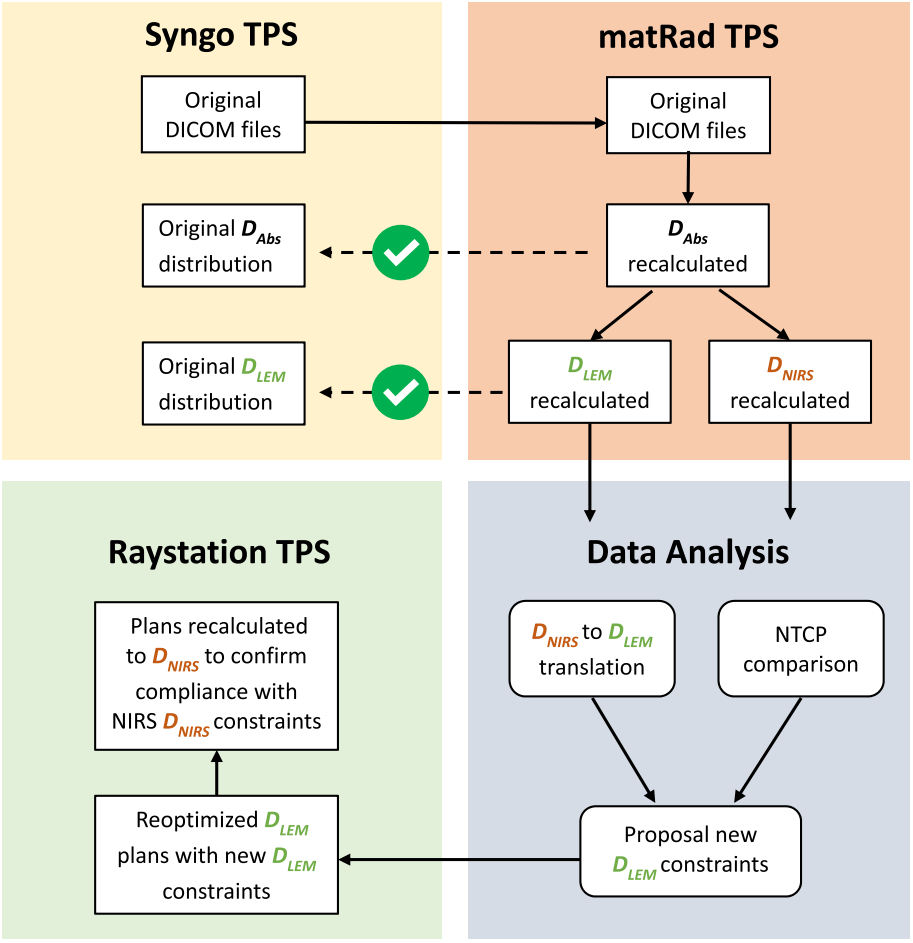

Fig. A1. Process of recalculation of RBE-weighted dose and proposal of new CNAO constraints. DICOM files from the original treatment plans were imported to the matRad TPS. The absorbed dose (D_{Abs}) and RBE-weighted dose distributions (D_{LEM} and D_{NIRS}) were recalculated. Correct reproduction of D_{Abs} and D_{LEM} compared to the original plans was confirmed. The recalculated D_{LEM} and D_{NIRS} were used for data analysis, in which new D_{LEM} constraints were proposed. Treatment plans were reoptimized with D_{LEM} in the RayStation TPS applying the new D_{LEM} constraints. Subsequently, these new plans were recalculated to D_{NIRS} to confirm that the plans still complied with the original NIRS constraints.

References

[1] Hasegawa A et al. Outcomes of visual acuity in carbon ion radiotherapy: analysis of dose-volume histograms and prognostic factors. Int J Radiat Oncol Biol Phys 2006;64:396–401.
[2] Kanai T et al. Biophysical characteristics of HIMAC clinical irradiation system for heavy-ion radiation therapy. Int J Radiat Oncol Biol Phys 1999;44:201–10.
[3] Kanai T et al. Irradiation of mixed beam and design of spread-out Bragg peak for heavy-ion radiotherapy. Radiat Res 1997;147:78–85.
[4] Kramer M, Scholz M. Treatment planning for heavy-ion radiotherapy: calculation and optimization of biologically effective dose. Phys Med Biol 2000;45:3319–30.
[5] Scholz M et al. Computation of cell survival in heavy ion beams for therapy. Radiat Environ Biophys 1997;36:59–66.
[6] Magro G et al. The FLUKA Monte Carlo code coupled with the NIRS approach for clinical dose calculations in carbon ion therapy. Phys Med Biol 2017.
[7] Fossati P et al. Dose prescription in carbon ion radiotherapy: a planning study to compare NIRS and LEM approaches with a clinically-oriented strategy. Phys Med Biol 2012;57:7543–54.
[8] Molinelli S et al. Dose prescription in carbon ion radiotherapy: how to compare two different RBE-weighted dose calculation systems. Radiother Oncol 2016;120:307–12.
[9] Steinstrater O et al. Mapping of RBE-weighted doses between HIMAC- and LEM-based treatment planning systems for carbon ion therapy. Int J Radiat Oncol Biol Phys 2012;84:854–60.
[10] Rossi S. The National Centre for Oncological Hadrontherapy (CNAO): status and perspectives. Phys Med 2015;31:333–51.
[11] Mirandola A et al. Dosimetric commissioning and quality assurance of scanned ion beams at the Italian National Center for Oncological Hadrontherapy. Med Phys 2015;42:5287–300.
[12] Common Terminology Criteria for Adverse Events v4.03. 2010, National Cancer Institute: NIH publication; no. 90-5410.
[13] Dale JE et al. Risk of carotid blowout after reirradiation with particle therapy. Adv Radiat Oncol 2017;2:465–74.
[14] Fukahori M et al. Estimation of late rectal normal tissue complication probability parameters in carbon ion therapy for prostate cancer. Radiother Oncol 2016;118:136–40.
[15] Shirai K et al. Dose-volume histogram analysis of brainstem necrosis in head and neck tumors treated using carbon-ion radiotherapy. Radiother Oncol 2017;125:36–40.
[16] Musha A et al. Prediction of acute radiation mucositis using an oral mucosal dose surface model in carbon ion radiotherapy for head and neck tumors. PLoS ONE 2015;10:e0141734.
[17] Shinoto M et al. Dosimetric analysis of upper gastrointestinal ulcer after carbon-ion radiotherapy for pancreatic cancer. Radiother Oncol 2016;120:140–4.
[18] Yanagi T et al. Dose-volume histogram and dose-surface histogram analysis for skin reactions to carbon ion radiotherapy for bone and soft tissue sarcoma. Radiother Oncol 2010;95:60–5.
[19] Jakel O et al. Treatment planning for carbon ion radiotherapy in Germany: review of clinical trials and treatment planning studies. Radiother Oncol 2004;73:S86–91.
[20] Schulz-Ertner D et al. Effectiveness of carbon ion radiotherapy in the treatment of skull-base chordomas. Int J Radiat Oncol Biol Phys 2007;68:449–57.
[21] Nikoghosyan AV et al. Randomised trial of proton vs. carbon ion radiation therapy in patients with low and intermediate grade chondrosarcoma of the skull base, clinical phase III study. BMC Cancer 2010;10:606.
[22] Lambrecht M et al. Radiation dose constraints for organs at risk in neuro-oncology; the European Particle Therapy Network consensus. Radiother Oncol 2018;128:26–36.